Impact of Layered Heterogeneity on Transient Saltwater Upconing in Coastal Aquifers

Antoifi Abdoulhalik[1,2*], Abdelrahman M. Abdelgawad [3], and Ashraf A. Ahmed[2]

[1] Civil Engineering Department, College of Engineering, Taibah University, Madinah, Saudi Arabia

[2] Department of Civil & Environmental Engineering, Brunel University London, Kingston Lane, Uxbridge UB83PH, UK

[3] Civil Eng. Department, Faculty of Engineering, Assiut University, Assiut, Egypt

*Corresponding author: Email: antoifi.abdoulhalik@gmail.com Tel. +33686468465

Abstract

This research investigated the effect of layered heterogeneity on transient saltwater upconing in a laboratory-scale coastal aquifer. The experiments were conducted in a 2D-laboratory flow tank, and the response of the saltwater wedge to pumping was analysed in a heterogeneous aquifer system, where a low permeability layer was constructed in the middle of the aquifer. The SEAWAT code was used for validation and to perform additional simulations to explore the sensitivity of the critical pumping rate and the critical time to the main parameters characterising the low-permeability layer, which included its permeability, thickness and position. The experimental results showed that the presence of layered heterogeneity noticeably altered the shape and the intrusion length of the upconing wedge without inducing a change in the abstraction rate "triggering" saltwater upconing mechanism compared to the homogeneous case. The numerical results of the layered aquifer provided excellent agreement with the experimental data for both the transient toe length and the shape of the steady-state saltwater wedges. The sensitivity analysis revealed that the critical pumping rate and the critical time was found to decrease considerably with decreasing hydraulic conductivity and thickness of the middle layer, which evidences the higher vulnerability of such layered aquifer systems to the saltwater upconing, in comparison to idealised homogeneous systems. The results nonetheless showed that varying the position of the

interlayer induced very little change on the critical pumping rate, but the critical time would tend to decrease as the low permeability layer was moved deeper away from the pumping well, particularly for smaller middle layer thickness.

Keywords: Seawater Intrusion; Saltwater Upconing; Aquifer salinisation; Laboratory experiments; Numerical modelling; SEAWAT

1. Introduction

The landward penetration of seawater in coastal aquifers, known as Seawater Intrusion (SWI), occurs mostly as a result of the over-exploitation the fresh groundwater. Also, factors related to climate change, which include the reduction in freshwater recharge (resulting from drought) and sea level rises, also severely enhance the intrusion mechanism, which subsequently leads to faster contamination. SWI can induce a substantial reduction of the fresh groundwater storage within the aquifer and ultimately lead to the salinization of pumping wells located nearby the coastline. The salinisation of the pumping wells occurs only by the mixing of 1% seawater (Abdoulhalik & Ahmed, 2018) and occurs as the freshwater-saltwater transition zone rise towards the bores of the wells, a mechanism called saltwater upconing (Reilly & Goodman, 1987).

The presence of inherent subsurface heterogeneity within the geological formation is an important factor affecting the saltwater intrusion mechanism. The presence of variations in the permeability within the subsurface not only causes the flow to be disrupted over various length scales, but also has a major contribution in density-dependent flow systems (Simmons et al., 2001; Houben & Post, 2017). The layered heterogeneous structures are amongst the most encountered forms of subsurface heterogeneity in real life aquifer systems. Many previous SWI studies have used such representations to simulate subsurface heterogeneous conditions (Ketabchi et al., 2014; Liu et al., 2014; Dose et al., 2014; Mehdizadeh et al., 2014; Mehdizadeh et al., 2017; Strack et al., 2015). Numerous experimental investigations have shown that layered heterogeneity considerably affects the position of the toe of the intruding wedge (Abdoulhalik & Ahmed, 2017a; Strack & Ausk, 2015) as well as the freshwater-saltwater transition-zone dynamics (Lu et al., 2013). Abdoulhalik and Ahmed (2017a) presented experimental evidence of the dependency of the rate of saltwater wedge motion (advancing and receding) as well as the widening of the transition-zone on the stratification pattern of the aquifer. While there is still a substantial need for further analyses of transient SWI in heterogeneous systems (Michael et al., 2017), studies investigating the sensitivity saltwater upconing mechanism to subsurface heterogeneity effects remain even scarcer.

The issue of saltwater upconing mechanism in coastal aquifer has recently been the topic of numerous investigations where idealised homogeneous condition was therein assumed (Johannsen et al., 2002; Mehdizadeh et al., 2015; Noorabadi et al., 2017; Stoeckl & Houben, 2012; Werner et al., 2009; Wirojanagud & Charbeneau, 1985; Zhou et al., 2005). Werner et al. (2009) evaluated the saltwater wedge response to various pumping regime and for saltwater densities. Stoeckl and Houben (2012) demonstrated that saltwater upconing mechanism was more sensitive to vertical pumping wells than horizontal pumping wells. Abdoulhalik and Ahmed (2018) examined the effect of hydraulic conductivity on the saltwater upconing mechanism. Their results evidenced that the upconing process was faster in low permeability aquifers. The higher vulnerability of low permeability aquifers to saltwater upconing was further demonstrated in Abdelgawad et al. (2018) . They investigated the influence of the pumping well design parameters (depth and location), the saltwater density and aquifer hydraulic conductivity and dispersivity on the critical pumping rate (abstraction rate prompting saltwater upconing mechanism) and the critical time (time taken for the saltwater to reach the well). Their results showed that the critical pumping rate was more sensitive to the variations in the well location than the pumping well depth. They also demonstrated that the critical pumping rate decreased with increasing saltwater densities while remaining relatively insensitive to dispersivity changes. While all these studies assumed homogenous conditions, an assessment of the impact of typical aquifer stratification on saltwater upconing mechanism and the associated transient related phenomena occurring within the rising freshwater-saltwater transition zone has never been provided.

Therefore, the aim of this study was to provide an insight into the effect of layered heterogeneity on the saltwater upconing mechanism, using laboratory and numerical modelling experiments. This study is a very first attempt to provide an insight on transience SWI under pumping conditions while incorporating in typical heterogeneous effects in laboratory-scale aquifer model. Several experiments were conducted on a layered aquifer where a low permeability (K) layer was set in the middle part of the aquifer. The objectives of this study were twofold: 1) to examine quantitatively and qualitatively the impact of layered heterogeneity on the temporal evolution of the shape and location of the upconing saltwater wedge in a laboratory-scale coastal aquifer system; 2) to explore the sensitivity of the critical pumping rate to the main parameters characterizing the heterogeneity effects, which included herein the middle layer permeability, its thickness and position into the aquifer. The laboratory experiments were conducted in a 2D flow tank where automated image analysis was implemented, and the SEAWAT code was used for numerical modelling.

2. Materials and methods

2.1 Experimental method

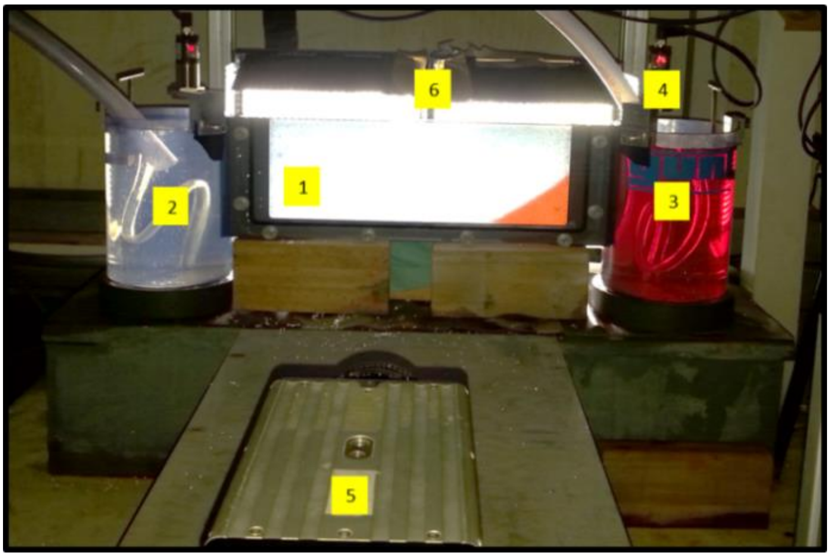

Figure 1 Photograph of the experimental setup; 1) porous media chamber; 2) freshwater reservoir; 3) saltwater reservoir; 4) ultrasonic sensors; 5) high-speed camera; 6) LED lights

The cross section of an unconfined coastal aquifer was simulated using a laboratory flow tank of dimension 0.38 m x 0.15 m x 0.01 m (Figure 1). The flow tank was composed by three distinct compartments: a central chamber and two circular side reservoirs. The porous media was simulated by filling the central chamber with clear glass beads from Whitehouse Scientific®. At the boundary between the central chamber and the side reservoirs were located fine mesh acrylic screens. The aperture diameter of these meshes was around 0.5 mm, which was sufficiently small to maintain the glass beads within the central chamber and large enough to enable the water to flow through.

Two different bead sizes were used in the experiments, namely 780 µm and 1090 µm. The hydraulic conductivity (K) of each was estimated using in situ measurement within the experimental flow tank using Darcy’s law, and the average hydraulic conductivity K were estimated at 85 cm/min and 36 cm/min, for the beads 1090 µm and 780 µm, respectively.

The heterogeneous case was simulated by forming a low K layer in the middle part of the aquifer using the beads of K = 36 cm/min. The thickness of the low K layer accounted for no more than one-third of the total saturated thickness of the aquifer that equalled h = 136 mm. The left and right side reservoirs were used to simulate constant freshwater-head and saltwater-head boundary conditions, respectively. The left side reservoir was filled with cold tap water, and the right side reservoir was filled with saltwater with a density of 1020 kg/m^3. The latter was dyed using red food colour to distinguish it from the freshwater.

The pumping well was simulated by inserting a needle vertically into the porous media which acted as a point sink. The needle was 50 mm long and was connected to a peristaltic pump (Watson Marlow 101 U/R) using a flexible hose. The internal diameter of the hose was 4.8 mm and was adjusted such that tip of the needle was located at 85 mm from the aquifer bottom (i.e. the bottom of the tank) and 190 mm away from the coastline (i.e. the boundary of the saltwater reservoir). Similar methods were used in Abdoulhalik & Ahmed (2018).

The saltwater intrusion experiment was initiated upon lowering the overflow outlet of the freshwater reservoir such that to impose an initial constant freshwater head of 135.7 mm while maintaining a constant saltwater head of 129.7 mm. This initial head boundary difference of dh = 6 mm (dh = 135.7-129.7= 6 mm), corresponded to a hydraulic gradient of 0.0158. This gradient is a typical value used in similar laboratory studies (Abdelgawad et al., 2018; Abdoulhalik & Ahmed, 2018) and within the range of values measured in some real coastal aquifers (Ferguson & Gleeson, 2012). This initial hydraulic gradient allowed the dense saline water to penetrate the porous media until the system reached steady state condition.

Once the initial steady state was established, the abstraction was initiated by switching on the pump. The pumping rate was first set to an initial rate of 0.09 mL/s and was after that gradually incremented by 0.1 mL/s. After each increment of the pumping rate, the system was allowed to reach a steady state condition. Once the saltwater upconing mechanism was observed, the critical pumping rate was recorded, and the pump was turned off. The same procedure was adopted in Abdoulhalik & Ahmed (2018). The images recorded throughout the experiments were after that post-processed such that the saltwater intrusion length could be calculated and the experimental images showing salt concentration distribution within the aquifer could be provided.

2.3 Numerical model and procedure

The MODFLOW variable-density flow code SEAWAT (Guo & Langevin, 2002) was selected for the numerical simulations. The porous media was represented by a rectangular model of dimensions 38 x 13 cm discredited uniformly using a size mesh of 0.2 cm. The longitudinal dispersivity was set at 0.1 cm, and the transverse dispersivity was considered to be 1/10 of the longitudinal dispersivity. The dispersivity values and the element dimensions satisfied the Peclet number criterion (Voss & Souza, 1987). Freshwater and saltwater (c = 28.96 g/l) hydrostatic boundary conditions were applied to the left and right sides of the porous media domain, respectively . The simulation time step was set to 0.5 min.

The initial condition of the model corresponded to an aquifer fully saturated with freshwater. The saline water penetrated the aquifer in the first stress period, as the freshwater and saltwater head boundaries were set at 13.57 cm and 12.97 cm, respectively. The pumping well was simulated at the design location, and the abstraction was initiated in the second stress period, with an initial discharge rate of 5.4 cm^3/min (i.e. 0.09 mL/s). The stress period was set to 50 min to allow the system to reach steady state. The discharge rate of the well was after that gradually incremented by 6 cm^3/min (i.e. 0.1 mL/s) until the saltwater upconing process was reproduced. The pumping rate was finally reset to zero. A summary of the parameters involved in the numerical simulations is shown in table 1.

Table 1 Summary of the numerical parameters

Input Parameters	Value
Domain length (cm)	38
Domain height (cm)	13
Element size (cm)	0.2
Hydraulic Conductivity (cm/min)	85
Porosity	0.3
Longitudinal dispersivity (cm)	0.1
Transversal dispersivity (cm)	0.01
Freshwater density (kg/m^3)	1000
Saltwater density (kg/m^3)	1020
Freshwater head (cm)	13.57
Saltwater head (cm)	12.97
Abstraction rates (mL/s)	0.49
Stress period (min)	50

3. Results and discussions

3.1. Saltwater upconing experiment

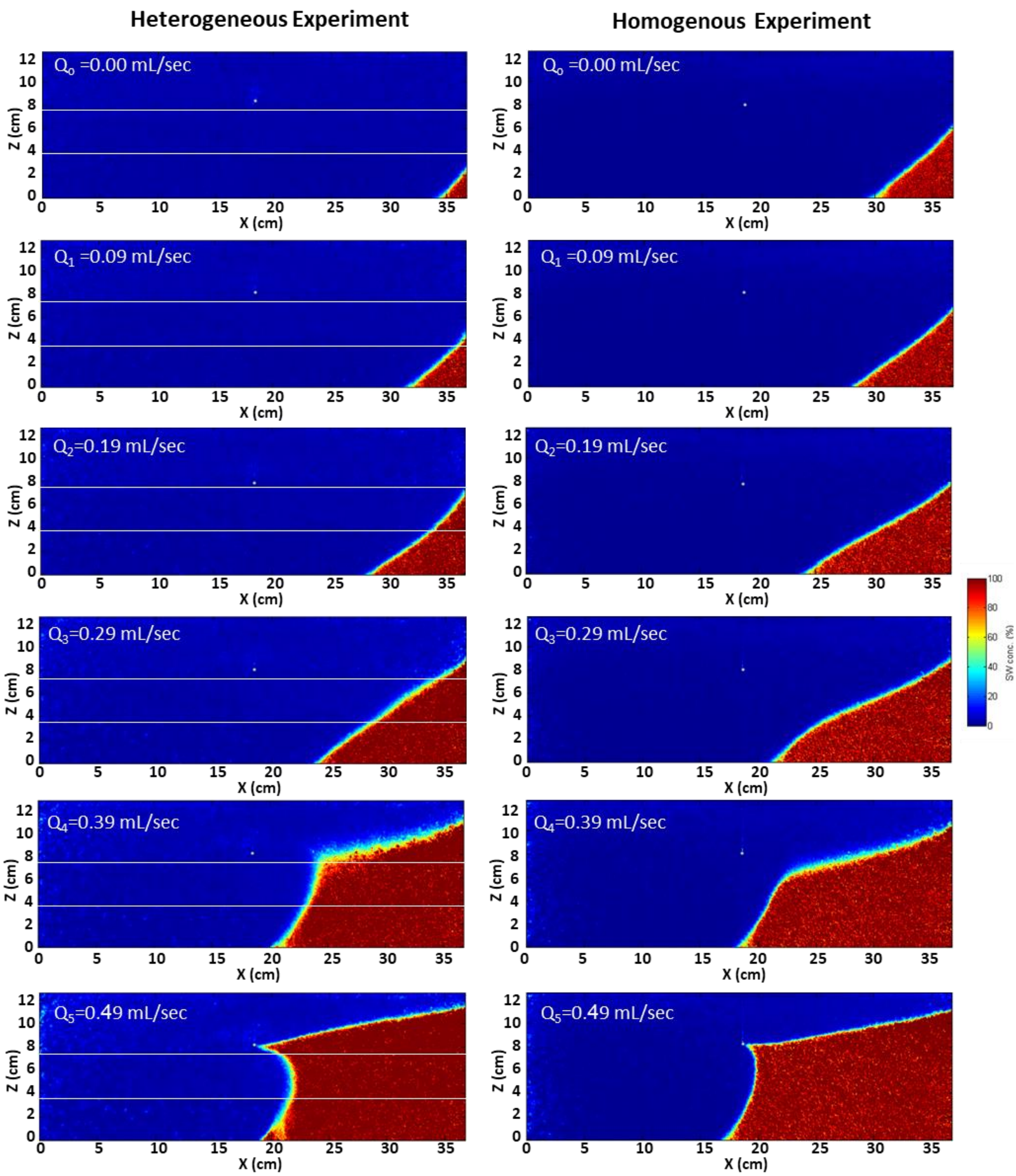

Figure 2. Experimental concentration colour maps showing the saltwater upconing process at different pumping rates in the heterogeneous case (left) and homogeneous case of Abdoulhalik and Ahmed (2018) (right)

The analysis of heterogeneity effects on saltwater upconing mechanism required the comparison of the heterogeneous results to data obtained in an identical aquifer but in homogeneous conditions, where the same hydrostatic boundary conditions and the same pumping rates were implemented. Therefore, the homogeneous results reported previously in Abdoulhalik & Ahmed (2018) were used here for comparison. Note that the hydraulic conductivity of the homogeneous case corresponded to the hydraulic conductivity of the1090µm beads used in the high K layers in the heterogeneous setting, as the size of the beads used in both cases was the same.

Figure 2 shows the steady-state concentration colour maps of the saltwater wedge at the various pumping rates for the heterogeneous and homogeneous cases. The initial intrusion length was visibly much smaller in the heterogeneous case for all the pumping rates tested. The saltwater intrusion length extended further inland as the abstraction was initiated. The toe length remained noticeably smaller in the heterogeneous case for all the pumping rates tested. The final upconing stage was considered when the freshwater/saltwater interface crossed the bore of the well, and the saltwater wedge reached steady state condition. Laboratory observations revealed that the abstraction rate that caused the occurrence of the saltwater upconing process was Q = 0.49 mL/s in both the heterogeneous and homogeneous cases. Figure 2 nonetheless shows that the intrusion length and the overall shape of the upconing wedge were somewhat altered by the presence of the middle low K layer in the heterogeneous case. The widening of the transition zone was therein noticeably greater, especially as the wedge approached the bore of the well (Q = 0.39 mL/s), and at the final upconing stage (Q = 0.49 mL/s) whereas it remained relatively thin in the homogeneous case. The final shape of the upconing wedge also exhibited a rather bulged shape in the top layer, while it appeared rather curved in the homogeneous case.

The values of each steady state toe length are given in table 2, and the transient toe length data are shown in Figure 3. The data show that the toe length values were greater as the pumping rate increased. The data also show that for equivalent pumping rate increment, the extent of the toe penetration of the saltwater wedge was smaller in the heterogeneous case compared to the homogeneous case. The difference decreased noticeably as the interface approached the well. The data show that the toe length was 49%, 34%, 17%, 9.4% and 10.7% greater in the homogeneous case than in the heterogeneous case, for Q = 0.09, 0.19, 0.29, 0.39, and 0.49 mL/s, respectively. Also, for equivalent pumping rate increment, figure 3 shows little difference in the toe migration rate between the heterogeneous and homogeneous cases, which indicates that the presence of the middle low permeability layer did not have a substantial effect on the sensitivity of the toe movement to modification of the pumping regime.

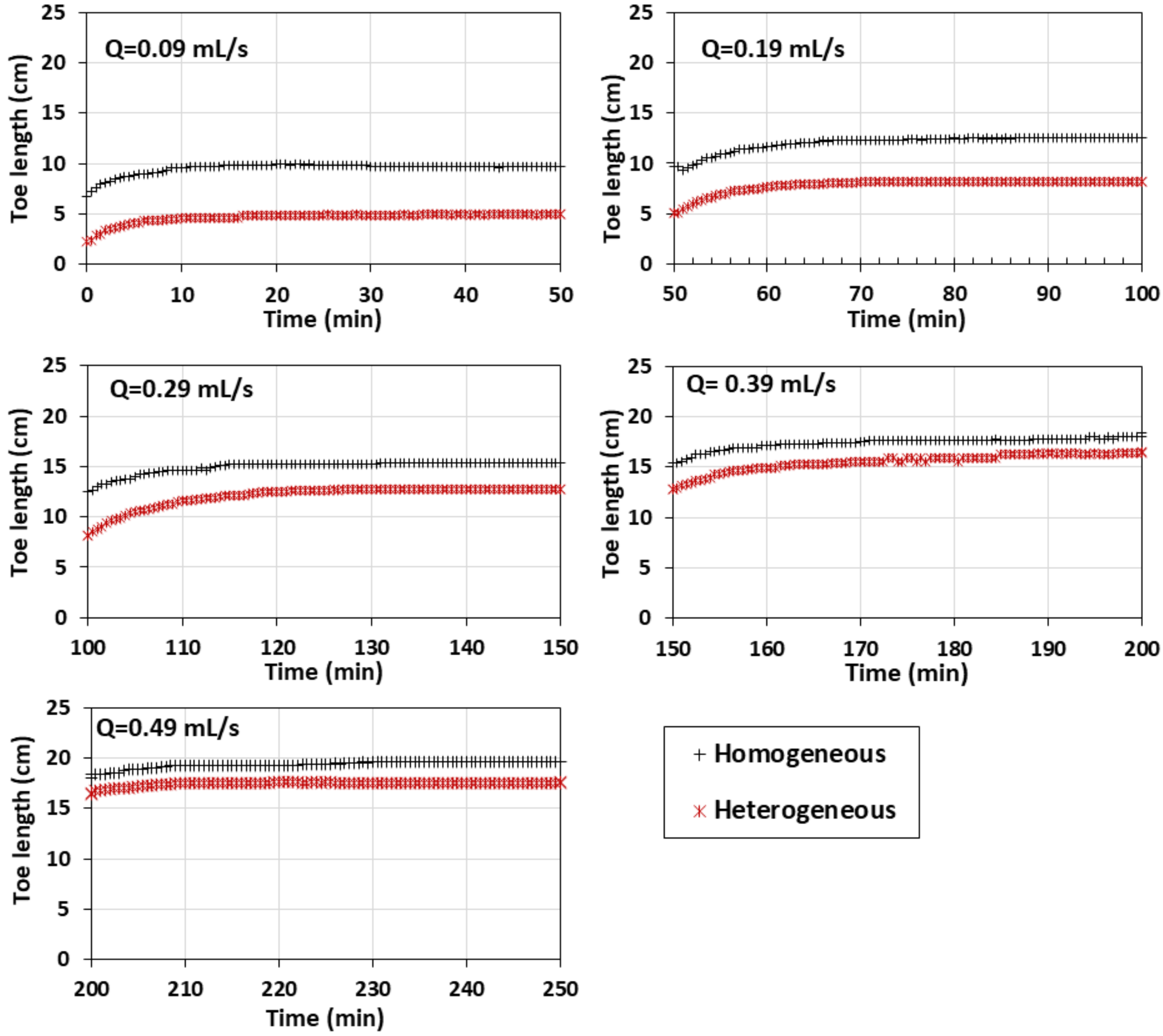

Figure 3. Transient experimental toe length data of the heterogeneous case (red points) and the homogeneous case of Abdoulhalik and Ahmed (2018) (black points)

Table 2 Steady-state toe length data in the heterogeneous case and the homogeneous case of Abdoulhalik and Ahmed (2018)

Pumping rate (mL/s)		0.09	0.19	0.29	0.39	0.49
Toe length (cm)	**Homogeneous**	9.8	12.5	15.4	18.0	19.6
	Heterogeneous	5	8.2	12.8	16.3	17.5

The experimental images of the receding saltwater wedge and the transient toe length data are shown in Figure 4. The figure shows that the interruption of the pump caused the seaward motion of the tip of the cone moved rapidly away from the well towards the seaside, with a substantial distortion of the wedge observed in the heterogeneous case. This delay was probably due to the slower repulsion of the saline water within the low permeability layer. The noticeable widening of the transition zone often associated with seawater retreat was visibly more pronounced in the heterogeneous case. Figure 5 shows that the migration rate of the toe of the saltwater wedge was nearly similar during the retreat, albeit somewhat faster in the heterogeneous case at the start, due to the slightly higher flow velocity at the bottom layer, as observed in previous studies (e.g. Abdoulhalik & Ahmed, 2017a).

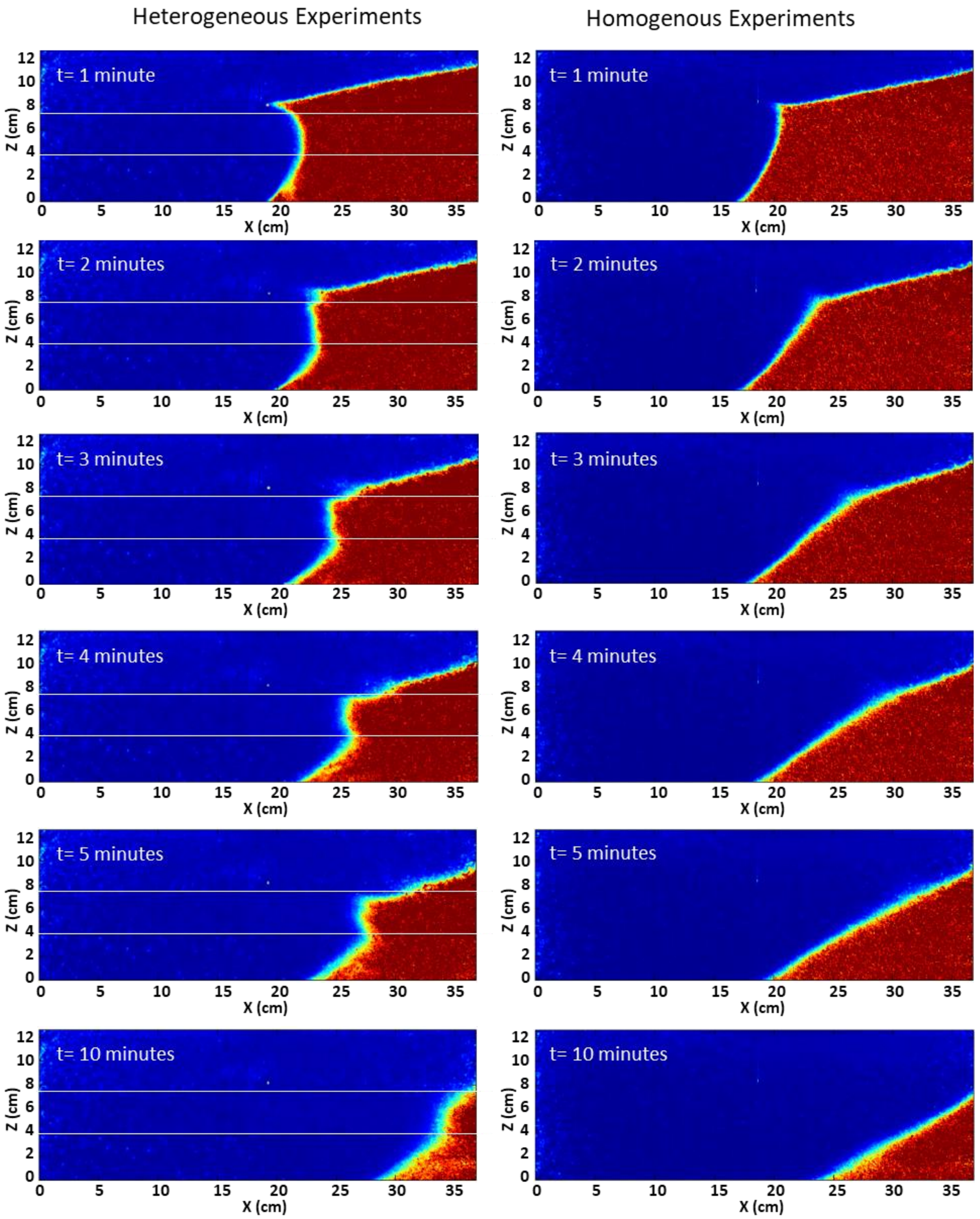

Figure 4. Experimental concentration colour maps of the receding process in the heterogenous case (left) and in the homogeneous case of Abdoulhalik and Ahmed (2018) (right)

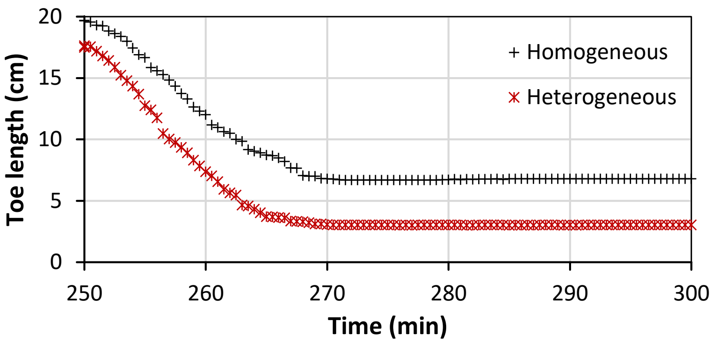

Figure 5. Toe length data of the receding wedge in the heterogeneous case (red points) and the homogeneous case of Abdoulhalik and Ahmed(2018) (black points)

3.2 Numerical modelling

The numerical model SEAWAT was used for the simulation of the experimental data of the heterogeneous scenario. The comparison was both qualitative (by comparing the saltwater wedge shape), and quantitative (by comparing the transient toe length data).

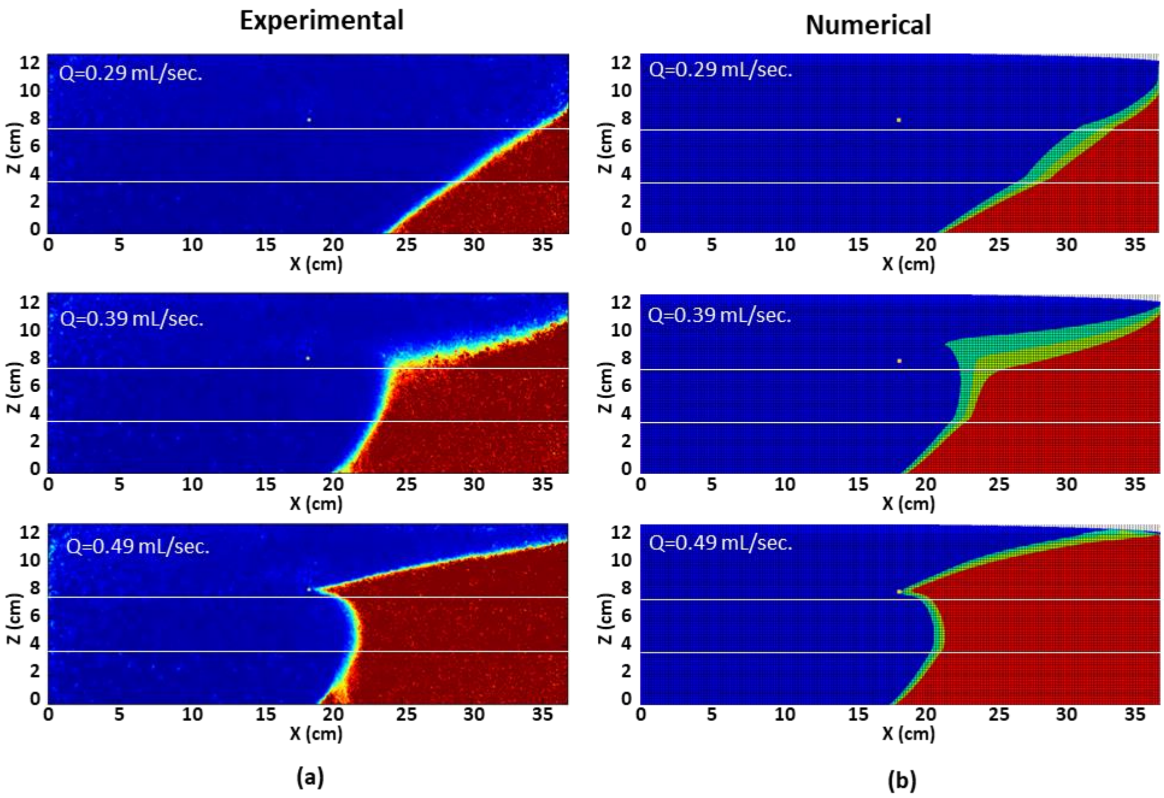

Figure 6 Comparison between the a) experimental and b) numerical steady-state saltwater wedges for Q = 0.29, 0.39, 0.49 mL/s in the heterogeneous case

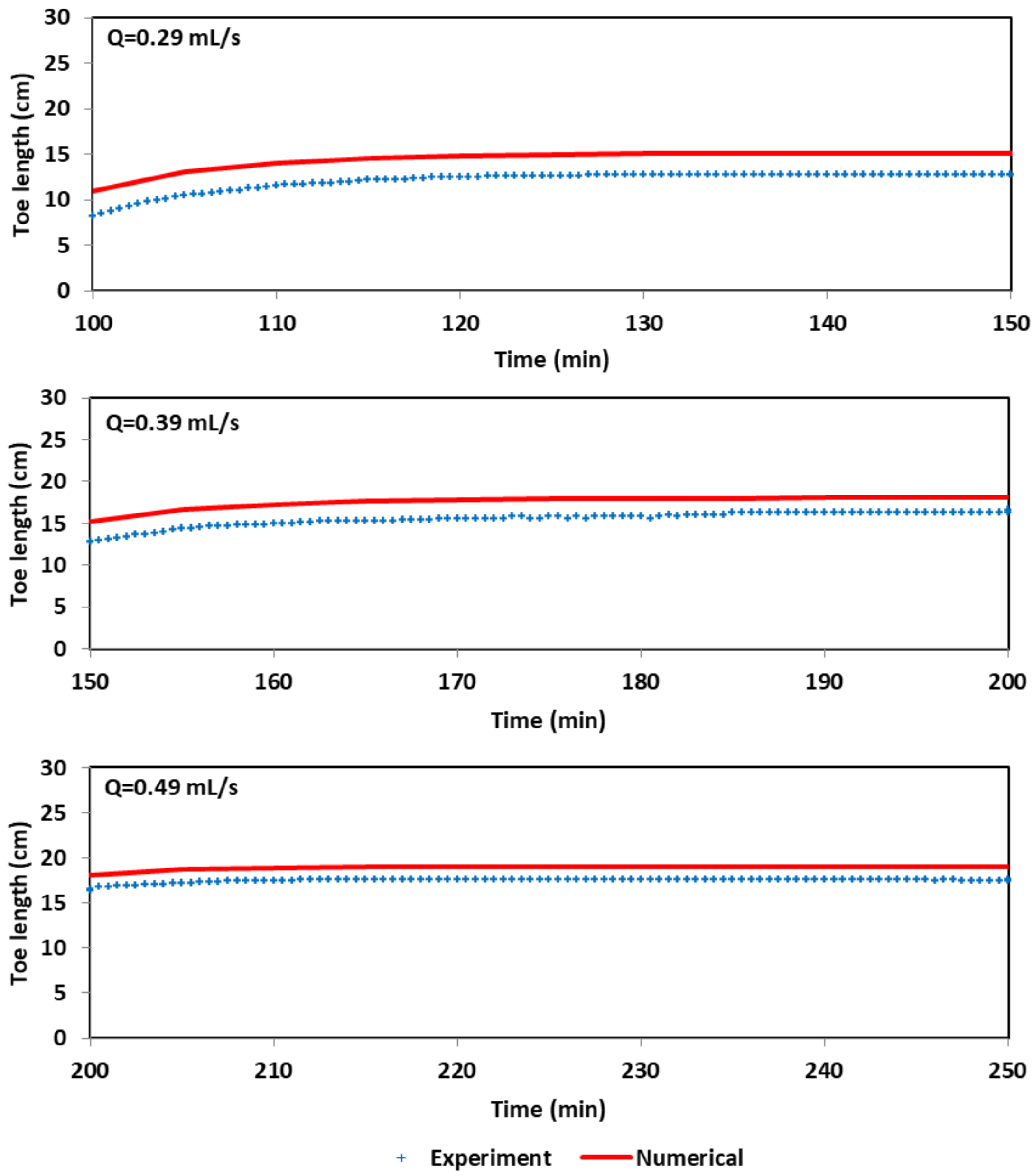

Figure 7. Comparison between the transient experimental and numerical model toe length data during abstraction for Q = 0.29, 0.39 and 0.49 mL/s in the heterogeneous case

Figure 6 compares the steady-state saltwater wedges for different pumping rates in the physical and numerical models. The results show that the numerical model could reproduce relatively well the overall shape of the saltwater wedge, albeit the widening of the transition zone within the low permeability layer was slightly more pronounced than in the physical model, especially before the upconing stage. The numerical model could predict relatively well the evolution from wide to thin transition zone conditions as the well reached upconing condition, in agreement with the experimental observations. The upconing wedge was relatively well depicted despite some minor visible discrepancies at the seaside boundary.

Figure 7 shows that the numerical model produced excellent matching with the physical experiment for the transient toe length data. The transient toe length was in overall slightly over-predicted in the numerical model. The percentage difference between experimental and numerical results was nonetheless fairly reasonable for each pumping rate, averaging maximum values of about 15%, 13% and 8% for Q = 0.29 mL/s, 0.39 mL/s and 0.49 mL/s, respectively. The comparison of the receding wedge toe length data following the interruption of the abstraction (i.e. Q = 0.0 mL/s) also shows good agreement (Figure 8b), particularly during the early stage of the retreat. The numerical model also depicted well the distortion of the saltwater wedge as well as the transition-zone widening during the receding motion, in agreement with the experimental observations (Figure 8a).

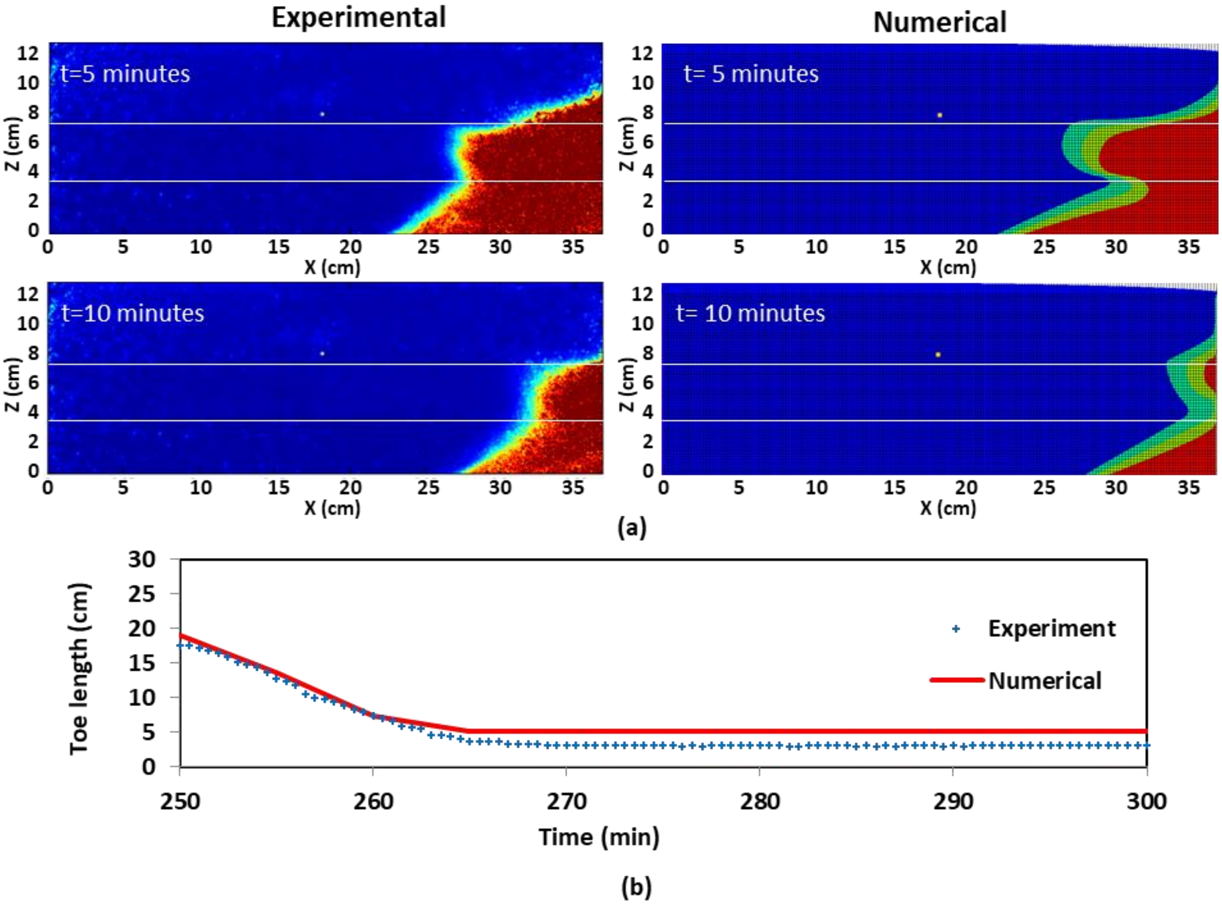

Figure 8 a) Comparison between experimental and numerical receding wedges following pumping shut off in the heterogeneous case; b) Comparison between transient experimental (blue points) and numerical (red line) toe length data in receding conditions in the heterogeneous case

4. Sensitivity analysis

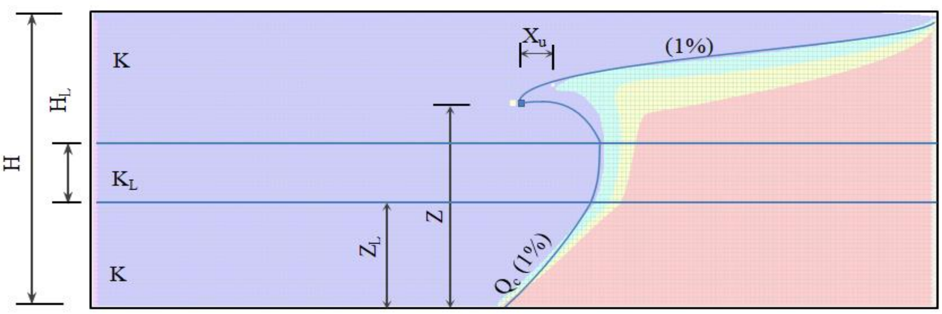

Figure 9 Schematic diagram of the saltwater upconing wedge in heterogeneous conditions

Additional simulations were completed to explore the influence of layered heterogeneity on the saltwater upconing mechanism. Specifically, the sensitivity of the critical pumping rate and the critical time to the main parameters characterising heterogeneity effects was quantitatively analysed. These parameters, which included the hydraulic conductivity of the middle layer (K_L), its thickness (H_L) and its position into the aquifer (Z_L), were investigated for two different pumping well positions. Figure 9 presents a schematic diagram of the aquifer system with the main parameters investigated herein. The critical pumping rate (Q_c) was considered as the minimal abstraction rate producing steady-state upconing such that the 1% salt contour line of the cone apex crosses the bore of the well. The critical time (t_c) was the time taken for the cone apex at 1% salt contour line to reach the well following the start of the abstraction (with $Q = Q_c$). The upconing distance (X_U), was introduced to refer to the horizontal distance between the apex of upconing at 1% salt contour line and the bottom of the well.

4.1 Effect of heterogeneity on the upconing distance with different well locations

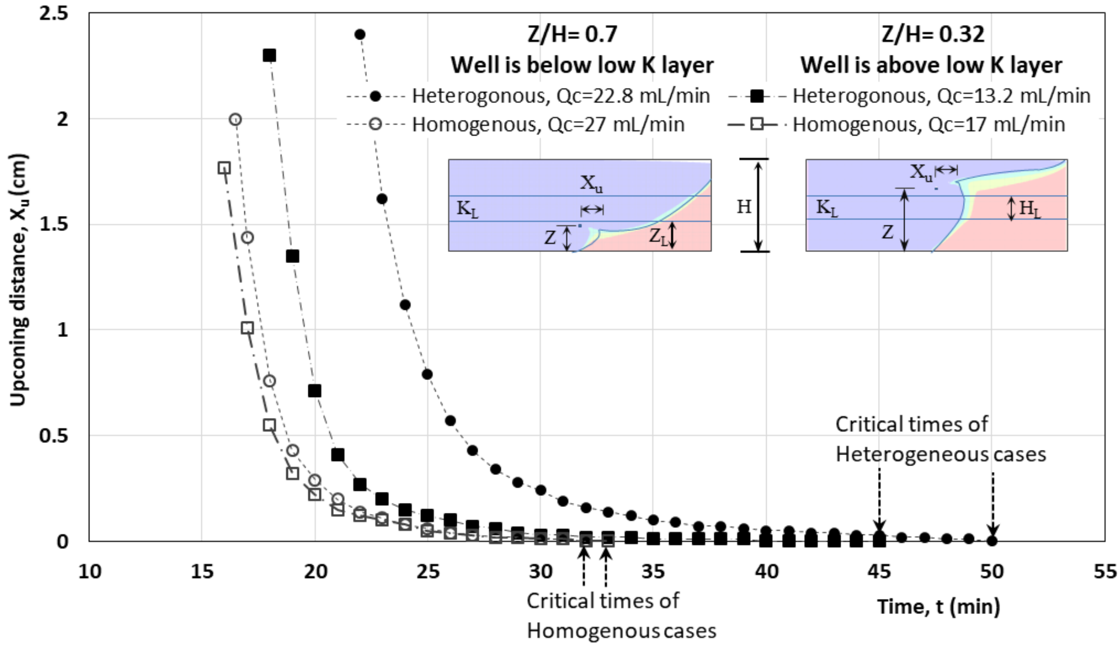

Figure 10 the effect of heterogeneity on the critical pumping rate and the occurrence of the upconing: Heterogeneous case (Kr=2.36, H_L/H =0.31 and Z_L/Z= 0.505)

Table 3 values of critical pumping rate in the homogenous and heterogeneous cases

	Shallow well (Z/H) = 0.7		Deep Well (Z/H) = 0.32	
	Homogenous	Heterogonous	Homogenous	Heterogonous
Critical pumping rate, Q_c (mL/min)	27	22.8	17	13.2

The comparison was made between homogenous and heterogeneous cases for two different pumping well positions, including Z/H = 0.7 (shallow well) and Z/H = 0.32 (deep well). In the heterogeneous case, the shallow well was located above the middle low K layer, while the deep well was located below the middle layer. The purpose of this sensitivity was to study the effect of heterogeneity on the critical pumping rate and to disseminate the upconing movement towards the well. The critical pumping rate for each case was found by trials and errors through several simulation runs using gradually increasing pumping rate.

Table 3 summarises the values of the critical pumping rates and Figure 10 shows the transient values of the upconing distance X_u in all the investigated cases, where decreasing X_u values characterise the movement of the saltwater towards the well. The effects of the pumping well depth on the time evolution of the upconing distance X_u was more pronounced in the heterogeneous scenario than in the homogeneous case, where very little changes could be observed. The results show that in the shallow and deep pumping scenarios, the critical pumping rate was noticeably lower in the heterogeneous cases compared to the homogeneous case. The presence of the low K middle layer induced a decrease of the critical pumping rate of about 16% and 22%, in the shallow and deep pumping scenarios, respectively. Hence, the results indicate that for the similar design well parameters, the presence of a low permeability layer increased the sensitivity of the well to saltwater upconing and therefore enhanced the vulnerability of the coastal aquifer system to the salinisation of production wells compared to the idealised homogeneous system.

4.2 Effect of the hydraulic conductivity contrast ratio

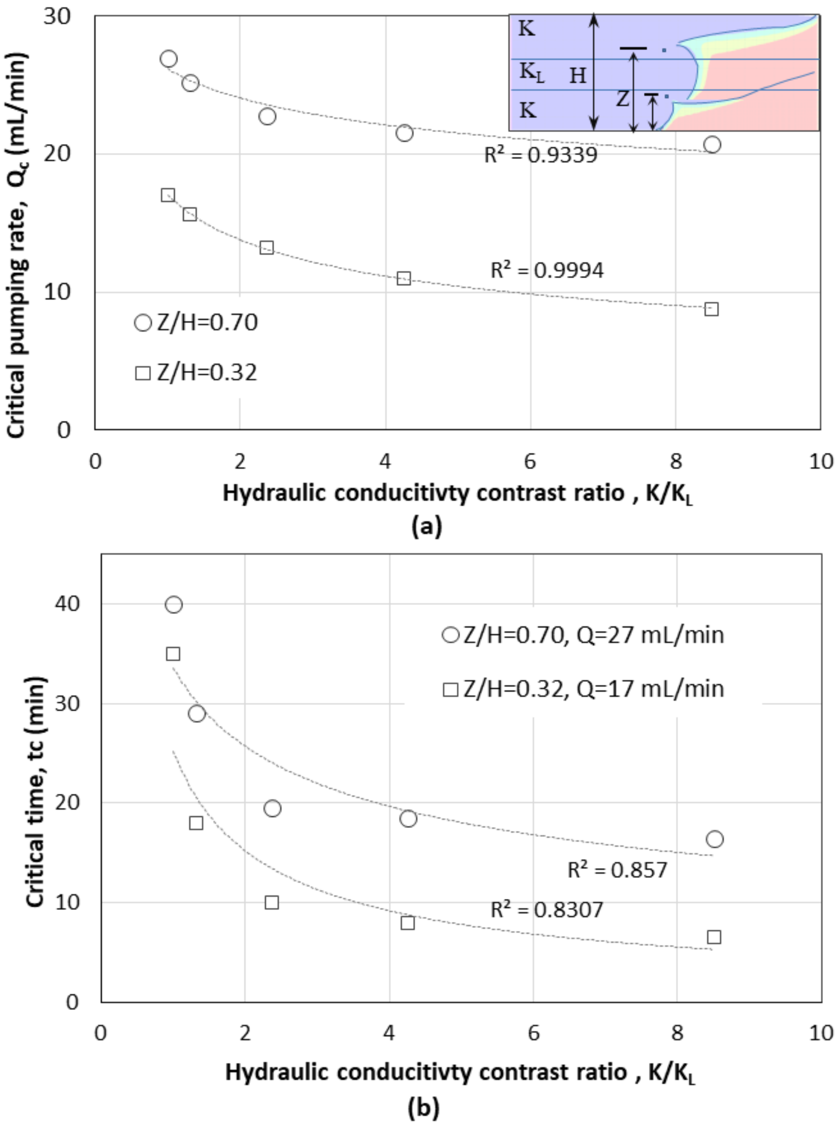

Figure 11 Effect of the hydraulic conductivity contrast ratio a) on the critical pumping rate b) on the critical time

Figure 11 shows the effect of the hydraulic conductivity of the middle layer that was examined for the shallow pumping well (Z/H = 0.7) and deep pumping well (Z/H = 0.32). The hydraulic conductivity of the middle layer was using the dimensionless ratio K/K_L, where K_L is the hydraulic conductivity of the middle layer K is the hydraulic conductivity of the top and bottom part of the aquifer (K = 85 cm/min). Five different permeability contrast ratio K/K_L were tested from 1 to 8.5, where K/K_L = 1 referred to the homogeneous condition.

The results show that the critical pumping rate significantly decreased with increasing permeability contrast (Figure 11a). The results show that from $K/K_L = 1$ to $K/K_L = 8.5$, the critical pumping rate decreased by 23% and 48%, for $Z/H = 0.7$ and $Z/H = 0.32$, respectively. Hence for a fixed well configuration and equivalent pumping rate increment, the saltwater upconing mechanism occurred faster for decreasing hydraulic conductivity of the middle layer. This may be because the freshwater flow contributing in the seaward repulsion of the saltwater wedge would tend to decrease as the permeability of the middle layer decreases, thereby leading to easier vertical migration of the saltwater wedge due to the abstraction, therefore a faster saltwater upconing mechanism. Hence, these results also suggest that the decreasing permeability of the middle layer substantially increases the vulnerability of the coastal aquifer system to pumping well salinisation through saltwater upconing mechanism. The impact of the middle layer permeability is higher during water abstraction from deep well than the one of the shallower well.

Also, the critical time was also found to noticeably decrease with increasing permeability contrast ratio K/K_L (Figure 11b). From the lowest to the highest K/K_L values tested, the critical time was decreased by 23 min. and 28 min, for $Z/H = 0.7$ and $Z/H = 0.32$, respectively. Note that to determine the critical time for each K/K_L scenario, the values of Q_c used for each well position corresponded to the values found for $K/K_L = 1$, at which the maximum value of the critical pumping rate occurred, such that to ensure the occurrence of the saltwater upconing mechanism in all cases.

4.3 The effect of low hydraulic conductivity layer thickness

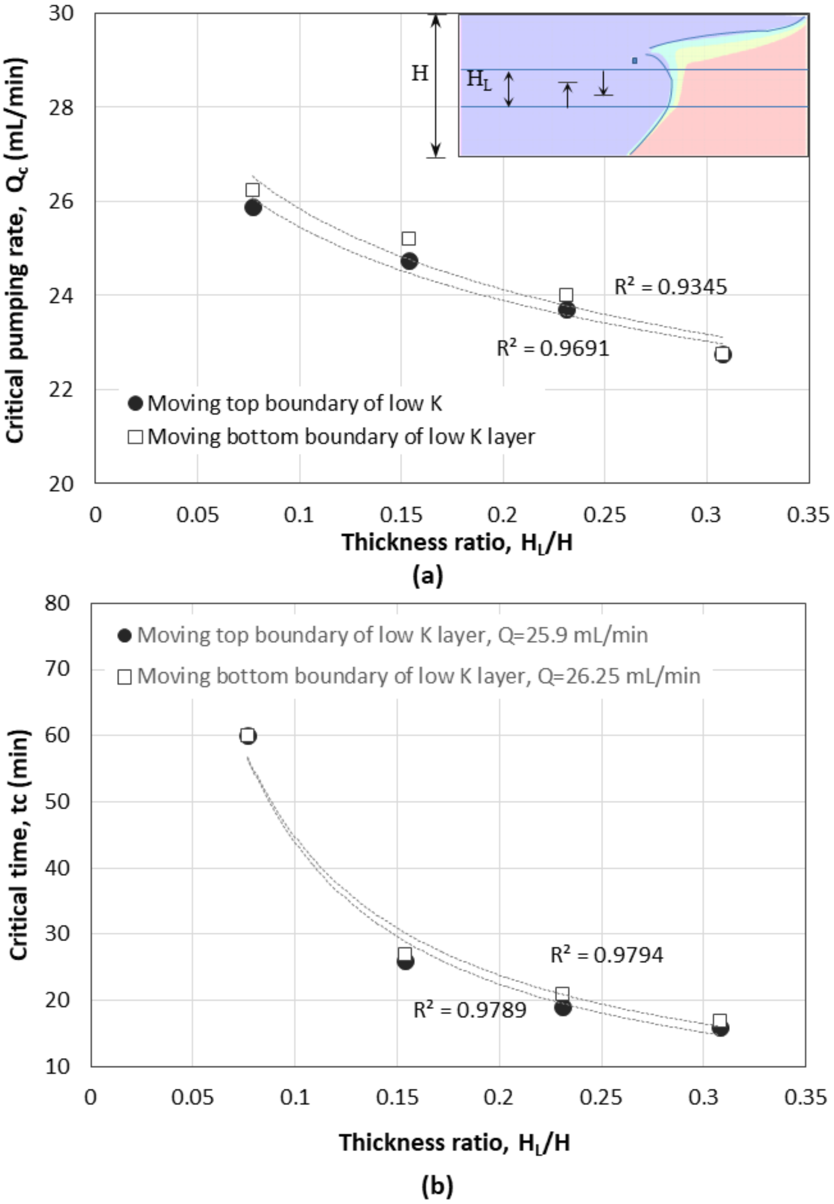

Figure 12 Effect of the middle layer thickness on a) the critical pumping rate and b) the critical time

Figure 12 shows the sensitivity of the critical pumping rate and the critical time to the thickness of the low K layer. The thickness of the middle layer was examined using the thickness ratio (H_L/H), where H_L is the thickness of the middle layer and H is the aquifer thickness (H = 13 cm). Two scenarios were tested: in the first, the top boundary of the low K middle layer was moved downwards; in the second scenario, the bottom layer was moved upwards.

Figure 12a shows that increasing thickness of the low K layer lowers the critical pumping rate, regardless of where the layer boundary change occurs. Therefore for equivalent pumping rate increment, larger the low permeability middle layer induced the earlier occurrence of saltwater upconing mechanism. From $H_L/H = 0.077$ to $H_L/H = 0.31$, the critical pumping rate decreased by 14% in the case where the top boundary was changed, while it decreased by 15 % when the bottom boundary was changed. These data show that the sensitivity of the critical pumping rate to the thickness ratio variations was nearly the same, whether the top boundary or the bottom boundary was changed.

The effect of thickness ratio on the critical time (Figure 12b) was investigated using the highest value of critical pumping rate for each respective scenario for all remaining thickness ratio. The data show that for a fixed pumping rate, the critical time considerably decreased as the thickness ratio H_L/H was increased. From the lowest to the highest H_L/H values tested, the critical time was decreased by almost 40 min in both the top and bottom boundary change scenarios, which clearly show that the increased thickness of the middle low K layer facilitated to saltwater upconing process, thereby inducing faster salinisation of the pumping well.

4.4 Effect of low K layer depth

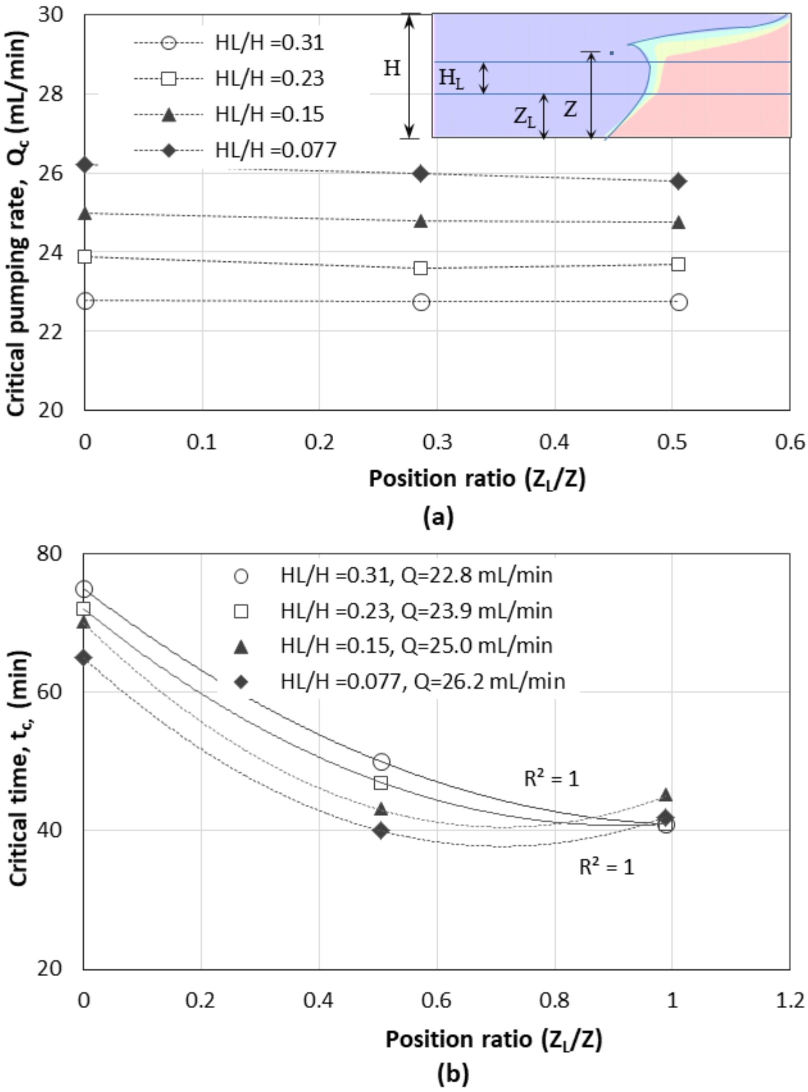

Figure 13 Effect of the low K layer position on a) the critical pumping rate and b) the critical time

Figure 13 shows the sensitivity of the saltwater upconing mechanism to the position of the low K layer. The position ratio (Z_L/Z) was considered to examine the effect of the varying the position of the middle layer, where Z_L is the distance between the bottom boundary of the middle layer and Z is the pumping well depth, the distance between the well and the aquifer bottom. Four different values of thickness ratio H_L/H were tested for the sake of completeness. The results show that varying the depth of low K layer caused negligible effects on the critical pumping rate (Figure 13a), but induced noticeable changes on the critical time (Figure 13b), which was found to decreases when the ratio Z_L/Z was increased, the critical time decreases. This means that as the low K layer was moved closer to the well, the saltwater upconing mechanism occurred faster, although this could not be observed for values of Z_L/Z exceeding 0.4 where the critical time slightly increased again particularly for $H_L/H = 0.23$ and $H_L/H = 0.31$.

5. Summary and conclusions

This investigation presented for the first time a quantitative analysis of the influence of layered heterogeneity on the saltwater upconing mechanism laboratory-scale unconfined coastal aquifer model. Physical experiments were first completed to observe the upconing process using automated image analysis. To quantify the effect of heterogeneity on the upconing process, the experimental results were compared to the data of the homogeneous case of Abdoulhalik & Ahmed (2018), that has similar hydrostatic conditions, and the same abstraction rates were used. The numerical model SEAWAT was used for validation, and the resulting model of the heterogeneouse scenario was used to perform additional simulations to explore the sensitivity of the critical pumping rate and the critical time to the main parameters characterising the middle layer, which included its permeability, its thickness and its position into the unconfined aquifer.

The experimental results showed that the presence of layered heterogeneity noticeably affected the shape and the intrusion length of the upconing wedge. The final shape of the upconing wedge in the heterogeneous case exhibited a wider transition-zone and a rather bulged shape, as opposed to the curved shape and the thin transition zone observed in the homogeneous case. Laboratory observations nonetheless showed that the saltwater upconing mechanism was "triggered" for the same abstraction rate as in the homogeneous case, for the pumping rate increment considered.

The numerical results of the heterogeneous unconfined aquifer model provided matched very well with the experimental data for both the transient toe length data and the shape of the steady-state saltwater wedges for different pumping rates. The sensitivity analysis performed using the resulting numerical model revealed that the critical pumping rate and the critical time was found to decrease considerably with decreasing hydraulic conductivity and thickness of the middle layer, which evidences the higher vulnerability to the saltwater upconing of coastal aquifer systems exhibiting layers of low permeability compared to an idealised homogeneous system. The results also showed that varying the position the interlayer induced very little change on the critical pumping rate, but the critical time would tend to decrease as the low permeability layer was moved deeper away from the pumping well, particularly for small values of middle layer thickness.

Acknowledgements

The experiments of this work were carried out at Queen's University Belfast when the first and third authors were associated with the institution.

References

Abdelgawad, A. M., Abdoulhalik, A., Ahmed, A. A., Moutari, S., & Hamill, G. (2018). Transient Investigation of the Critical Abstraction Rates in Coastal Aquifers: Numerical and Experimental Study. *Water Resources Management*, *32*(11), 3563–3577. https://doi.org/10.1007/s11269-018-1988-3.

Abdoulhalik, A., & Ahmed, A. A. (2017). How does layered heterogeneity affect the ability of subsurface dams to clean up coastal aquifers contaminated with seawater intrusion? *Journal of Hydrology*, *553*(September), 708–721. https://doi.org/10.1016/j.jhydrol.2017.08.044.

Abdoulhalik, A., & Ahmed, A. A. (2018). Transient investigation of saltwater upconing in laboratory-scale coastal aquifer. *Estuarine, Coastal and Shelf Science*, *214*(June), 149–160. https://doi.org/10.1016/j.ecss.2018.09.024.

Dose, E. J., Stoeckl, L., Houben, G. J., Vacher, H. L., Vassolo, S., Dietrich, J., & Himmelsbach, T. (2014). Experiments and modeling of freshwater lenses in layered aquifers: Steady state interface geometry. *Journal of Hydrology*. https://doi.org/10.1016/j.jhydrol.2013.10.010

Ferguson, G., & Gleeson, T. (2012). Vulnerability of coastal aquifers to groundwater use and climate change. *Nature Climate Change*, *2*(5), 342–345. https://doi.org/10.1038/nclimate1413.

Guo, W., & Langevin, C. D. (2002). *User's Guide to SEAWAT: A computer program for simulation of three-dimensional variable-density ground-water flow*. *USGS Techniques of Water Resources Investigations*.

Houben, G., & Post, V. E. A. (2017). The first field-based descriptions of pumping-induced saltwater intrusion and upconing. *Hydrogeology Journal*, *25*(1), 243–247. https://doi.org/10.1007/s10040-016-1476-x.

Johannsen, K., Kinzelbach, W., Oswald, S., & Wittum, G. (2002). The saltpool benchmark problem - Numerical simulation of saltwater upconing in a porous medium. *Advances in Water Resources*, *25*(3), 335–348. https://doi.org/10.1016/S0309-1708(01)00059-8

Ketabchi, H., Mahmoodzadeh, D., Ataie-Ashtiani, B., Werner, A. D., & Simmons, C. T. (2014). Sea-level rise impact on fresh groundwater lenses in two-layer small islands. *Hydrological Processes*, *28*(24), 5938–5953. https://doi.org/10.1002/hyp.10059.

Liu, Y., Mao, X., Chen, J., & Barry, D. A. (2014). Influence of a coarse interlayer on seawater intrusion and contaminant migration in coastal aquifers. *Hydrological Processes*. https://doi.org/10.1002/hyp.10002.

Lu, C., Chen, Y., Zhang, C., & Luo, J. (2013). Steady-state freshwater-seawater mixing zone in stratified coastal aquifers. *Journal of Hydrology*, *505*, 24–34. https://doi.org/10.1016/j.jhydrol.2013.09.017.

Mehdizadeh, S. S., Werner, A. D., Vafaie, F., & Badaruddin, S. (2014). Vertical leakage in sharp-interface seawater intrusion models of layered coastal aquifers. *Journal of Hydrology*, *519*(PA), 1097–1107. https://doi.org/10.1016/j.jhydrol.2014.08.027

Mehdizadeh, S. S., Vafaie, F., & Abolghasemi, H. (2015). Assessment of sharp-interface approach for saltwater intrusion prediction in an unconfined coastal aquifer exposed to pumping. *Environmental Earth Sciences*, *73*(12), 8345–8355. https://doi.org/10.1007/s12665-014-3996-9.

Mehdizadeh, S. S., Karamalipour, S. E., & Asoodeh, R. (2017). Sea level rise effect on seawater intrusion into layered coastal aquifers (simulation using dispersive and sharp-interface approaches). *Ocean & coastal management*, *138*, 11-18.

Michael, H. A., Post, V. E., Wilson, A. M., & Werner, A. D. (2017). Science, society, and the coastal groundwater squeeze. *Water Resources Research*, *53*(4), 2610-2617.

Noorabadi, S., Nazemi, A. H., Sadraddini, A. A., & Delirhasannia, R. (2017). Laboratory investigation of water extraction effects on saltwater wedge displacement. *Global Journal of Environmental Science and Management-Gjesm*, *3*(1), 21–32. https://doi.org/10.22034/gjesm.2017.03.01.003.

Reilly, T. E., & Goodman, A. S. (1987). Analysis of saltwater upconing beneath a pumping well. *Journal of Hydrology*, *89*(3–4), 169–204. https://doi.org/10.1016/0022-1694(87)90179-X

Simmons, C. T., Fenstemaker, T. R., & Sharp, J. M. (2001). Variable-density groundwater flow and solute transport in heterogeneous porous media: Approaches, resolutions and future challenges. *Journal of Contaminant Hydrology*. https://doi.org/10.1016/S0169-7722(01)00160-7.

Stoeckl, L., & Houben, G. (2012). Flow dynamics and age stratification of freshwater lenses: Experiments and modeling. *Journal of Hydrology*, *458*, 9–15. https://doi.org/10.1016/j.jhydrol.2012.05.070.

Strack, O. D. L., & Ausk, B. K. (2015). A formulation for vertically integrated groundwater flow in a stratified coastal aquifer. *Water Resources Research*, *51*(8), 6756-6775.

Voss, C. I., & Souza, W. R. (1987). Variable density flow and solute transport simulation of regional aquifers containing a narrow freshwater-saltwater transition zone. *Water Resources Research*, *23*(10), 1851–1866. https://doi.org/10.1029/WR023i010p01851

Werner, A. D., Jakovovic, D., & Simmons, C. T. (2009). Experimental observations of saltwater up-coning. *Journal of Hydrology*, *373*(1–2), 230–241. https://doi.org/10.1016/j.jhydrol.2009.05.004.

Wirojanagud, P., & Charbeneau, R. J. (1985). Saltwater upconing in unconfined aquifers. *Journal of Hydraulic Engineering*, *111*(3), 417–434. https://doi.org/10.1061/(ASCE)0733-9429(1985)111:3(417).

Zhou, Q., Bear, J., & Bensabat, J. (2005). Saltwater upconing and decay beneath a well pumping above an interface zone. *Transport in Porous Media*, *61*(3), 337–363. https://doi.org/10.1007/s11242-005-0261-4.